Oualid AMIEUR[1]*, Fatiha ZIDANI[2]

Department of Electrical Engineering, Laboratory LSPIE, University of Batna-2, Algeria. (1*,2).

doi: 10.15199/48.2022.02.05

A Robust Voltage H_∞ Controller in DG-Connected Inverter Based on Auto-Calibration of Adjustable Fractional Weights

Abstract. *In this paper a H_∞ control technique addresses the voltage regulation in distributed generation (DG) system connected to power converter under harmonic disturbances. The DG control technique combines a discrete sliding mode control (DSMC) in the current control and a Robust Servomechanism Problem (RSP) in the voltage control. Besides, a fractional Order Proportional-Integral-Derivative (FOPID) controller synthesized with an automatic calibration of adjustable fractional weights is formulated in this work. For performance and high robustness requirements, the parameters of FOPID are optimized through solving a multiobjective optimization problematic based on the automatic calibration of the weighted-mixed sensitivity problem. Furthermore, for ensuring an adequate calibration of parameters, the Integral of Time Weighted Absolute Error (ITAE) criterion with Genetic Algorithm (GA) are used to achieve better voltage regulation. The simulation results show that it can achieve trade-off between nominal performance (NP) and robust stability (RS) margins for the constrained uncertain plants in the large range frequencies. Also, the results validate the effectiveness of the proposed control at which both low total harmonic distortion (THD) and low tracking error.*

Streszczenie. *W niniejszym artykule technika sterowania H_∞ dotyczy regulacji napięcia w systemie generacji rozproszonej (DG) podłączonym do przekształtnika mocy w warunkach zakłóceń harmonicznych. Technika sterowania łączy dyskretne sterowanie w trybie ślizgowym (DSMC) w sterowaniu prądem i solidny problem z serwomechanizmem (RSP) w sterowaniu napięciem. Poza tym, w niniejszej pracy sformułowano regulator ułamkowo-całkująco-różniczkujący (FOPID) zsyntetyzowany z automatyczną kalibracją regulowanych mas ułamkowych. Parametry FOPID są optymalizowane poprzez rozwiązanie problemu optymalizacji wielokryterialnej opartej na autokalibracji problemu wrażliwości mieszanej ważonej dla wymagań dotyczących odporności między nominalną wydajnością (NP), solidną stabilnością (RS) marżami i kompromisem między nimi w dużych zakres częstotliwości. Wyniki symulacji potwierdzają skuteczność proponowanego sterowania, przy którym zarówno wysoka odporność, jak i niskie całkowite zniekształcenia harmoniczne (THD).**(Stabilny regulator napięcia H_∞ w energetyce rozproszonej - podłączony falownik oparty na autokalibracji regulowany mas ułamkowych)***

Keywords: Fractional Order, Weighted-Mixed Sensitivity, Power Converter, DG System, THD, Stability Analysis
Słowa kluczowe: Porządek ułamkowy,Czułość ważona mieszana,Konwerter napięcia,DG System,THD,Analiza stabilności

Introduction

A The nonlinear loads such as non-sinusoidal currents and voltages, power electronic converters, high-speed semiconducting switches and solid state drives were the major causes for harmonics in the small DG sources (solar power, wind power, etc.) increasing the reactive power and affecting badly to the power networks [1]. The international $IEEE-519$ standards impose a limit value less than 5% of global THD [2]. In the literature, different control techniques of DG-connected inverter have been proposed, where a high-quality voltage with low THD is needed to cover with basic and advanced control strategies.

The most basic and commonly used control structure for DG-connected inverter including two loops: current control loop and secondary voltage and frequency control loop [3]. For a fixed model of the system, the performance of the controller is very high. However, the RS control need to the exact model with parametric uncertainty to achieve the both performances of low THD and fast dynamic response [4].

The voltage control with considering the uncertainty has been widely addressed in the literature such as; Baghaee et al [5] presented a generalized H_∞ control. Marwali et al [6] It has developed an RSP controller based on an uncertain plant model. Hornik et al [7] introduced a H_∞ based on repetitive control to improve the tracking performance, low THD and protection from peak-current. Sedghi et al [8] proposed an H_∞ based control method to adjust the MG under the uncertainties of the load changes. Grundling et al [9] a RS adaptive control for uninterruptible power supplies (UPS) is developed. Sheela et al [10] applied H_∞ control to optimize voltage and frequency deviations after load changing. Lee et al [11] proposed RS analysis with H_∞ loop-shaping controller for UPS under perturbation. Mohamed[12] proposed an RS controller for a current source inverter based on H_∞ and μ-analysis techniques. Lam et al [13] developed a robust multi-variable H_∞ controller using LMI technique and a μ-synthesis. Zhao et al [14] used the PSO technique to optimize the weighting function of the H_∞ controller. Pe et al [15] applies the H_∞ RS controller design method in the Matlab Robust Control Toolbox for high frequency resonant inverters but includes only load and external input voltage in the perturbation. Bevrani, et al [16] applies an LMI based μ-synthesis that shows more robustness compared to the conventional H_∞ control. Maniza, et al [4] proposed a linear matrix inequality approach to satisfy the Lyapunov stability criterion. Hamzeh, et al [17], extend the nonconvex optimization problem to the LMI conditions for voltage regulation, including the uncertainties of the system parameters. Raeispour, et al [18] and Gholami, et al [19], a robust mixed H_2/H_∞ control strategies has been proposed based on multiobjective optimization. D'Arco, et al [20] designs PI-based schemes for fast dynamic compensation, protection versus overcurrent and low THD.

The recorded control strategies cannot achieve the desired optimum trade-off between NP and RS when the model uncertainties are taken into account in the control parameters. To overcome this vulnerability, Sedraoui et al [21] use weighted-mixed sensitivity problem by proposing adjustable fractional weights. In general, the complementary sensitivity plot is obtained when the maximal singular values vanish as much as possible at high frequencies and approach unity at low frequencies. Amieur et al [22] proposed more analysis using a PSO optimization algorithm to guaranty optimal adjustable fractional weights. So that, the voltage control of the DG-connected inverter can be formulated as solving the weighted-mixed sensitivity problem. To the best of our knowledge, this research will use the typical $FOPID$ in the voltage control loop using H_∞ structures, which is inspired by the robustness of the fractional $FOPID$, a promising approach for solving the weighted-mixed sensitivity problem and ensure a good trade-off between NP and RS for the nominal and uncertainty plants, in which the adjustable weight is calibrated for getting the desired form of load voltage.

System Modeling, Control and Stability Analysis

The DG-connected inverter system used in this paper consists of a 3-phases voltage converter with $L^{\smile}C$ filter and a Δ-Y transformer. Figure 1 shows a circuit diagram of the system. Small capacitors C_{load} at the load side to provide further harmonics filtering and stabilization of the load voltages. The line-to-neutral load voltages are denoted as $\vec{V}_{load}$ and load currents $\vec{I}_{load}$, the line-to-line inverter filter capacitor voltages are denoted as $\vec{V}_f$ and the inverter currents are denoted as $\vec{I}_f$. The DG bus voltage through the individual inverter is assumed to be an ideal DC voltage source. The leakage inductance L_t, series resistance R_t and currents I_{snd} are the secondary winding parameters [23, 24].The control technique developed in this work is based on the technique proposed by Marwali [6].

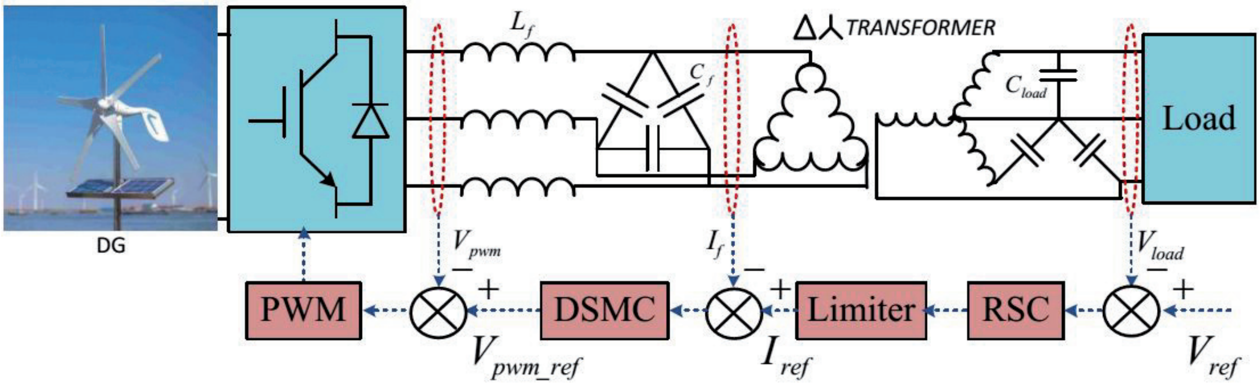

Fig. 1. DG-connected inverter model.

As shown in Figure 1, a dual-loop control structure is used, where the inner loop is for current control ($DSMC$) and the outer loop for voltage control based on RSP controller. The RSP is based on the solution of the servomechanism problem [23] where they combined between internal model principle [24] and the optimal control theory. The RSP is designed taking the dynamics of the $DSMC$ into account. The state space form of the dynamic equations is,

(1) $$\begin{cases} \dot{x}(t) = Ax(t) + Bu(t) + Ed(t) \\ y(t) = Cx(t) \end{cases}$$

where

$$A = \begin{bmatrix} 0_{2\times2} & (3C_f)^{-1}.I_{2\times2} \\ -(L_f)^{-1}.I_{2\times2} & 0_{2\times2} \end{bmatrix}, B = \begin{bmatrix} 0_{2\times2} \\ (L_f)^{-1}.I_{2\times2} \end{bmatrix},$$

$$C = \begin{bmatrix} -(3C_f)^{-1}.T_{ri_{dq}} \\ 0_{2\times2} \end{bmatrix}.$$

The states are $x = \begin{bmatrix} V_{f_{qd}} & I_{f_{qd}} \end{bmatrix}^T$, the control inputs $u = \vec{V}_{pwm_{qd}}$, disturbance $d = \vec{I}_{snd_{qd}}$ and output to be regulated $y(t)$. The system can be converted to a discrete time system with constant sampling time T_s to yield,

(2) $$\begin{cases} x(k+1) = A^*x(k) + B^*u(k) + E^*d(k) \\ y(k) = Cx(k) \end{cases}$$

For designing the $DSMC$ controller the surface is chosen as $s(k) = Cx(k) - I_{ref_{qd}}(k)$, where $Cx(k) = I_{f_{qd}}(k)$,so that when sliding mode occurs, $s(k) = 0$ or $I_{f_{qd}}(k) = I_{ref_{qd}}(k)$. The control is given as,

(3) $$V_{pwm_{qd}}(k) = (CB^*)^{-1}(I_{ref_{qd}} - CA^*x(k)) - CA^*d$$

The current command $I_{ref_{qd}}$ limited in magnitude. The errors between the inverter current commands and the actual inverter commands,

(4) $$e_{I_{qd}} = I_{ref_{qd}} - I_{f_{qd}}$$

The $DSMC$ will force these errors to zero by computing the necessary voltage commands given by (3). To design the RSP voltage controller we need to consider a combination of the true plant in (2) and the $DSMC$ (4) as the "equivalent plant" . The controller is given by states feedback,

(5) $$I_{ref_{qd}}(k) = K_0x_p(k) + K_1\eta(k)$$

where the states x_p the augmented true plant for $DSMC$.

The states η represents implementation of the continuous transfer function $\frac{1}{s^2+\omega_i^2}$, where $\omega_i = 2\pi f_i$ with $i = 1, 3, \ldots$ represents the fundamental frequency to track and the harmonic frequencies to be eliminated.The gains $K = [K_0, K_1]$ are found by minimizing a certain linear quadratic cost function for the augmented "equivalent plant" and a discrete form of the servo-compensator:

(6)
$$\begin{bmatrix} x_p(k+1) \\ \eta(k+1) \end{bmatrix} = \begin{bmatrix} A_d & 0 \\ -B_c^*C & -A_c^* \end{bmatrix} \begin{bmatrix} x_p(k) \\ \eta(k) \end{bmatrix} + \begin{bmatrix} B_d \\ -B_c^*D \end{bmatrix} u(k)$$

For the goal of stability analysis of the $MIMO$ linear system under structured perturbations, a structured singular value μ can be used. The problem is depicted in Figure 2, where M denotes a known stable $MIMO$ transfer function with W inputs and Z outputs and Δ a structured uncertainty matrix.

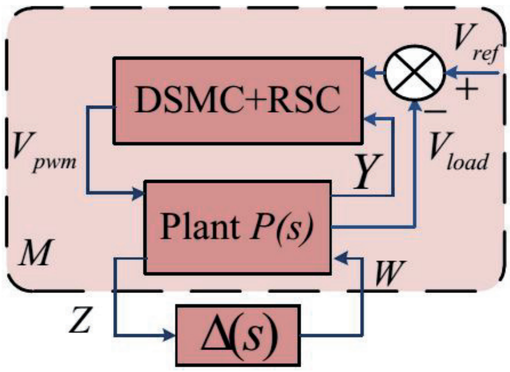

Fig. 2. Uncertain closed-loop model.

The structured singular value of M with respect to the uncertainty set Δ is defined as,

(7)
$$\mu_\Delta(M) = \frac{1}{min\{\delta(\Delta_i) : \Delta_i \in (\Delta), det(I - M\Delta_i = 0)\}}$$

The generalized small-gain theorem provides RS results of the system using the structured singular value. It states that if nominal $M(s)$ is stable then the perturbed system $(I-M\Delta)^{-1}$ is stable for all stable Δ_i for which $\|\Delta_i\|_\infty \leq 1$ and only if $\mu_\Delta(M(j\omega)) < 1$ for all $\omega \in R$.

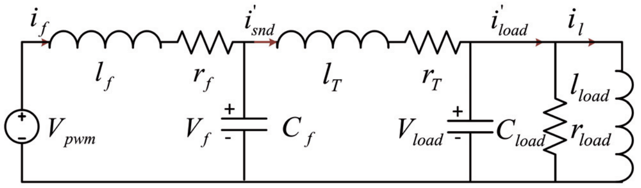

Fig. 3. Open-loop model of the nominal plant.

The linear fractional transformations (LFT) can be used to achieve the RS based on $\mu - framework$ analysis. The problem needs to be recast to that of Figure 2. Using the model (1), a single-phase equivalent circuit of the converter with RL load can be derived as shown in Figure 3. The dynamic equations of the plant are given as [6],

$$\text{(8)} \qquad \begin{cases} \frac{dv_f}{dt} = \frac{(i_f - i'_{snd})}{C_f} \\ \frac{di_f}{dt} = \frac{(-r_T i_f - v_f - v_{pwm})}{l_T} \\ \frac{dv_{load}}{dt} = \frac{i'_{snd} - g_{load} v'_{load} - i_L}{C_{load}} \\ \frac{di'_{snd}}{dt} = \frac{(-r_T i'_{snd} + v_f - v'_{load})}{l_T} \\ \frac{di_L}{dt} = \lambda_{load} v'_{load} \\ i'_{load} = g_{load} v'_{load} + i_L \end{cases}$$

where $g_{load} = \frac{1}{r_{load}}$ is the per-unit conductance of the load and $\lambda_{load} = \frac{1}{l_{load}}$ is the inverse of the load inductance.

$P_{ind} = \{, c_f, l_f, c_{load}, l_T, r_f, r_T, g_{load}, \lambda_{load}\},$, the above parameters can be represented as parametric output multiplicative uncertainties using lower $LFTs$ with the uncertain perturbation δ blocks separately can be precisely written as follows form:

$$\text{(9)} \qquad P_{ind} = P_{ind0}(1 + \tau_{P_{ind}} \delta_{P_{ind}}), |\delta_{P_{ind}}| < 1$$

Where, $\Delta(s) = \{\delta_{c_f}, \delta_{l_f}, \delta_{c_{load}}, \delta_{l_T}, \delta_{r_f}, \delta_{r_T}, \delta_{g_{load}}, \delta_{\lambda_{load}}\}$.

By inspection, the nominal plant's state space model is given as,

$$\text{(10)} \qquad \begin{cases} \dot{X}(t) = AX_p(t) + B_p U(t) \\ Y(t) = C_p X(t) + D_p X(t) \end{cases}$$

States: $X = \begin{bmatrix} V_f & I_f & v_{load} & i_{snd} & i_L \end{bmatrix}^T$,

Inputs: $U = \begin{bmatrix} v_{pwm} & W^T \end{bmatrix}^T$

$W = \begin{bmatrix} w_{c_f}, w_{l_f}, w_{c_{load}}, w_{l_T}, w_{r_f}, w_{r_T}, w_{g_{load}}, w_{\lambda_{load}} \end{bmatrix}^T$,

Outputs: $Y = \begin{bmatrix} v_f & v_f & v_{load} & i_{load} & Z^T \end{bmatrix}^T$,

$Z = \begin{bmatrix} z_{c_f}, z_{l_f}, z_{c_{load}}, z_{l_T}, z_{r_f}, z_{r_T}, z_{g_{load}}, z_{\lambda_{load}} \end{bmatrix}^T$,

$$A_p = \begin{bmatrix} A_{nom} \end{bmatrix}, B = \begin{bmatrix} B_{nom} & B_{del} \end{bmatrix}, C = \begin{bmatrix} C_{nom} \\ C_{del} \end{bmatrix},$$

$$\mathrm{D}_p = \begin{bmatrix} D_{nom} \\ D_{del} \end{bmatrix}.$$

The terms with subscription nom and del are the nominal model parameters derived from (7). The nominal open-loop plant (combination of $P(s)$ and $\Delta(s)$) and the closed controller loop make up the system $M.Matlab'ssysic$ command has been utilized for this transformation.

In order to speed up the response and improve the transient performance of the DG system, a local controller is developed by solving the H_∞ optimization problem. Therefore, to have a better voltage tracking, the gains associated with the outer-loop can be estimated by introducing adjustable fractional weights.

Fractional H_∞ Mixed Sensitivity Control for Voltage Loop Development

The formulation of optimization problem can be posed under the general H_∞ control configuration. The robust control strategies have been proposed to determine the parameters of a robust controller. The optimal H_∞ control problem with this configuration consists a minimizing of iteration process the ratio γ between the energy of the vector Z and the energy of the vector W. The implementation of the iteration process with various well-known software packages such as [25, 26]. The fractional-order controller to be synthesized $K(s,x) \in \square^{m \times m}$ is parameterized by the vector that will be determined later by optimization tools. Such a controller has the following form, which can be arranged in a matrix form as,

(11)

$$K(s,x) = \begin{bmatrix} K_{11}(s,x) & K_{12}(s,x) & \cdots & K_{1m}(s,x) \\ K_{21}(s,x) & K_{22}(s,x) & \cdots & K_{2m}(s,x) \\ \vdots & \vdots & \ddots & \vdots \\ K_{m1}(s,x) & K_{m2}(s,x) & \cdots & K_{mm}(s,x) \end{bmatrix}$$

with:

$$\text{(12)} \qquad K_{ij}(s,x) = K_{p_{ij}} + \frac{K_{i_{ij}}}{s^{\lambda_{ij}}} + K_{d_{ij}} s^{\mu_{ij}}$$

Yields also the following design parameter vector:

$$\text{(13)} \qquad x = \begin{bmatrix} K_{p_{ij}}, K_{i_{ij}}, K_{d_{ij}}, \lambda_{ij}, \mu_{ij} \end{bmatrix}$$

The transfer function of the closed loop above-mentioned system can be derived as,

$$\text{(14)} \qquad T_{zw} = \begin{bmatrix} W_s(s)S(s) \\ W_T(s)T(s) \end{bmatrix}$$

The terms $W_s(s)$ and $W_T(s)$ are the tracking performance and stability weighting matrices, respectively. The very general guidelines for weighting matrices choice were proposed in [27, 28, 29] and were used in this paper, though were not strictly followed:

$$\text{(15)} \qquad W_s(s) = \left(\frac{\frac{s}{\sqrt{M_s}} + \omega_B^*}{s + \omega_B^* A_s} \right) I_{m \times m}$$

,

$$W_T(s) = \left(\frac{\frac{s}{\omega_{BT}^*} + \frac{1}{\sqrt{M_T}}}{\frac{A_T s}{\omega_{BT}^*} + 1} \right) I_{m \times m}$$

In order to secure the suitable RS, complimentary sensitivity transfer matrix $T(s,x)$ has been used. For acquiring the NP the sensitivity transfer matrix $S(s,x)$, has been used. This characteristic can be obtained by defining a performance weighting matrices to shape the sensitivity function. In the mixed sensitivity problem, both conditions are combined in order to determine the robust performance (RP) condition.

$$\text{(16)} \qquad \underbrace{\overbrace{\|W_s(j\omega)S(j\omega,x)\|_\infty}^{NB} + \overbrace{\|W_T(j\omega)T(j\omega,x)\|_\infty}^{RS}}_{RP} \leq 1$$

Therefore, we want to satisfy (16):

$$\text{(17)} \qquad min_{x\in\chi}\left\|\begin{matrix} W_s(s)S(s,x) \\ W_T(s)T(s,x)\end{matrix}\right\|_\infty \Leftrightarrow$$

$$min_{x\in\chi}\left(max_\omega\left(\sigma_{max}\begin{bmatrix} W_s(j\omega)S(j\omega,x) \\ W_T(j\omega)T(j\omega,x)\end{bmatrix}\right)\right)$$

In this work, We use conventional and structured H_∞ techniques available in $Matlab$, such as $HinfLMI$ and $Hinfstruct$, to synthesize the robust voltage H_∞ controller and solve problem (17).

Consider a general class of $SISO$ nth order nonlinear systems given by the following nonlinear state space; where M_s and M_T are high frequency gains,A_s and A_T are low frequency gains and ω_B^* and ω_{BT}^* determine crossover frequency. Next, p and n denote the order of a function should be kept as low as possible [27]. In this paper, $\omega_s(s,\grave{p})$ is the performance weighting function that is specified for the disturbance elimination to restrict the magnitude of the sensitivity function and $\omega_T(s,\grave{n})$ the robustness weighting function is identified for the uncertainty in the plant to limit the magnitude of the complementary sensitivity function. This approach, known as loop shaping, is frequently used for choosing the weight functions for controller synthesis.

$$\text{(18)} \qquad W_s(s,\grave{p}) = \left(\frac{\frac{s^{\grave{p}}}{\sqrt{M}_s}+\omega_B^*}{s^{\grave{p}}+\omega_B^* A_s}\right) I_{m\times m},$$

$$W_T(s,\grave{n}) = \left(\frac{\frac{s^{\grave{n}}}{\omega_{BT}^*}+\frac{1}{\sqrt{M}_T}}{\frac{A_T s^{\grave{n}}}{\omega_{BT}^*}+1}\right) I_{m\times m}$$

If $S(s,x)$ indicates the plant sensitivity function (transfer function between output and disturbance) and $T(s,x)$ represents the plant's complimentary sensitivity function (transfer function output/input). Therefore, the multiobjective optimization problem can be expressed as follows,

$$\text{(19)} \qquad \begin{cases} \bar{\sigma}[\,S(j\omega,x)] \, < \bar{\sigma}[\,W_s^{-1}(j\omega)] \\ \bar{\sigma}[\,T(j\omega,x)] \, < \bar{\sigma}[\,W_T^{-1}(j\omega)] \\ \bar{\sigma}[\,W_s^{-1}(j\omega)] \, + \bar{\sigma}[\,W_T^{-1}(j\omega)] \, \geq 1 \end{cases}$$

In the mixed sensitivity problem, we want to satisfy:

$$\text{(20)} \quad \bar{x} = [\,x,\grave{n},\grave{p}] \, \in \bar{\chi} = [\,\bar{x_1}^-,\bar{x_1}^+]\,x...x[\,\bar{x_n}^-,\bar{x_n}^+]$$

$$\text{(21)} \qquad min_{\bar{x}\in\bar{\chi}}\left\|\begin{matrix} W_s(s,\grave{n})S(s,x) \\ W_T(s,\grave{p})T(s,x)\end{matrix}\right\|_\infty \Leftrightarrow$$

$$min_{\bar{x}\in\bar{\chi}}\left(max_\omega\left(\sigma_{max}\begin{bmatrix} W_s(j\omega,\grave{n})S(j\omega,x) \\ W_T(j\omega,\grave{n})T(j\omega,x)\end{bmatrix}\right)\right)$$

In the design procedure, parameters of the $FOPID$ controller can be defined as a variable vector $x = [\,K_{p_{ij}}, K_{i_{ij}}, K_{d_{ij}}, \lambda_{ij}, \mu_{ij}]$, where each component is constrained by:

$$\text{(22)} \qquad \begin{cases} K_{p,i,d_{min}} \leq K_{p,i,d} \leq K_{p,i,d_{max}} \\ \lambda_{min} \leq \lambda \leq \lambda_{max} \\ \mu_{min} \leq \mu \leq \mu_{max} \end{cases}$$

The idea is to determine the previous optimal parameters using GA optimization algorithm and based on the minimization of the criterion $ITAE$ that is expressed by Equation (22) as,

$$\text{(23)} \qquad ITAE = \int_{t_0}^{t_f} t|V_{ref}(t) - V_{load}(t,x)|dt$$

where t_0 and t_f are the start and end times of simulation. The objective function in Matlab is defined by conceding the voltage deviations betweenV_{load} and V_{ref} in terms of the temporal characteristics that provide the GA with a reasonable tracking error.

Simulation Results

The proposed robustification approach is simulated using two steps. The first is constructed using typical integer weights, and their RS, NP, and RP robustness margins are then improved by automatic calibration of adjustable fractional weights. The first step of simulation permits defining frequency space and different rules for formulation of fractional weighted-mixed sensitivity problem. Subsequently, for improving the RP margins, an optimization algorithm is used to enhance the NP-RS trade-off. Performance of the proposed steps is evaluated using simulation in MATLAB/Simulink environment. The parameters are presented in Table 1.

Table 1. System Parameters.

Parameters	Values
DG voltage V_{dc}	540V
AC Output voltage V_{load}	208V(LL), 120V(LN)
Filter capacitance C_f	540μF
Filter inductance l_f	300 μH
Transformer inductance l_T	48 μH
Transformer resistance r_T	0.02 Ohm
Transformer ratio	245 :208 V
System frequency f	60 Hz
Load side capacitors C_{load}	90 μF

For the robust voltage H_∞ controller, the system provided through classical H_∞ based-$LMIs$ function MATLAB software. The GA search space of $FOPID$ controller optimal parameters is chosen as,

$$\text{(24)} \qquad \begin{cases} 0.01 \leq K_{p,i,d} \leq 10 \\ 0.001 \leq \lambda \leq 0.99 \\ 0.001 \leq \mu \leq 0.99 \end{cases}$$

For the Closed-loop system performance specifications,we select the search space of weighting functions parameters as follow,

$$\text{(25)} \qquad \begin{cases} 0.01 \leq \omega_B^*, \omega_{BT}^* \leq 100 \\ 0.01 \leq M_s, M_T \leq 5 \\ 0.01 \leq A_s, A_T \leq 10 \\ 0.01 \leq \grave{p}, \grave{n} \leq 0.99 \end{cases}$$

Where the parameters of the GA are selected by:

- $Generationnumber = 30;$
- $Tolerancefunction = 10^{-4};$
- $Populationsize = 30;$
- $Plotfunction : @gaplotbestfun.$

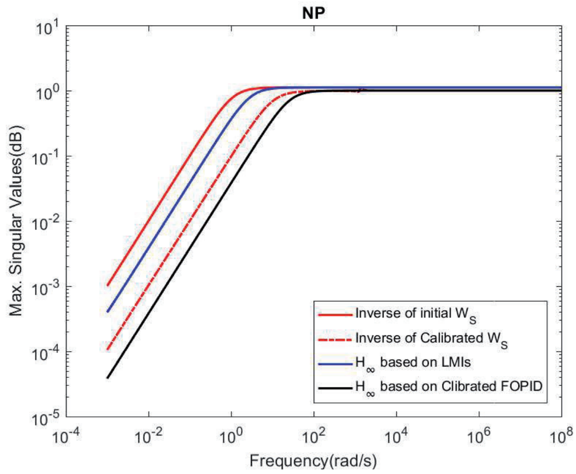

Fig. 4. Singular values of the NP margin.

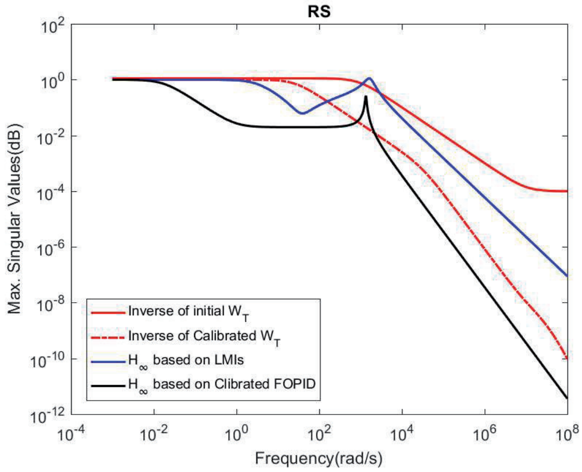

Fig. 5. Singular values of the RS margin.

In designing the robust voltage controller, the tracking performance weighting matrices are chosen as,

(26)
$$W_s(s) = \left(\frac{\frac{s}{\sqrt{1.12}}+2.6}{s+2.6*0.99}\right) I_{2\times 2}, W_T(s) = \left(\frac{\frac{s}{3.37}+\frac{1}{\sqrt{1.12}}}{\frac{0.58s}{3.37}+1}\right) I_{2\times 2}$$

where $M_s = 1.12$, $\omega_B^* = 2.6 rad/s$, $A_s = 0.99$ for transfer function of the NP weight and $M_T = 1.12$, $\omega_{BT}^* = 3.37 rad/s$, $A_T = 0.58$ for transfer function of the RS weight. The optimization process is repeated 23 times with different initial populations due to the $GA's$ deterministic structure. As a consequence, after the fourth iteration, the optimal reduction achieves the required level, with the fitness function attenuated below one (0.8993). Furthermore, the given optimal solution allows determining the performance and sensitivity weighting functions respectively as follow:

(27)
$$W_s(s, \grave{p}^{best}) = \left(\frac{\frac{s^{0.5412}}{\sqrt{1.12}}+2.60}{s^{0.5412}+2.60*8.0076}\right) I_{2\times 2},$$

$$W_T(s, \grave{n}^{best}) = \left(\frac{\frac{s^{0.5313}}{3.378}+\frac{1}{\sqrt{1.25}}}{\frac{2.8244 s^{0.5313}}{3.378}+1}\right) I_{2\times 2}$$

Where

$$\begin{cases} 0.01 \le \omega_B^* = 2.60 \le 100 \\ 0.01 \le \omega_{BT}^* = 3.378 \le 100 \\ 0.01 \le M_s = 1.12 \le 5 \\ 0.01 \le M_T = 1.25 \le 5 \\ 0.01 \le A_s = 8.0076 \le 10 \\ 0.01 \le A_T = 2.8244 \le 10 \\ 0.01 \le \grave{p} = 0.5412 \le 0.99 \\ 0.01 \le \grave{n} = 0.5313 \le 0.99 \end{cases}$$

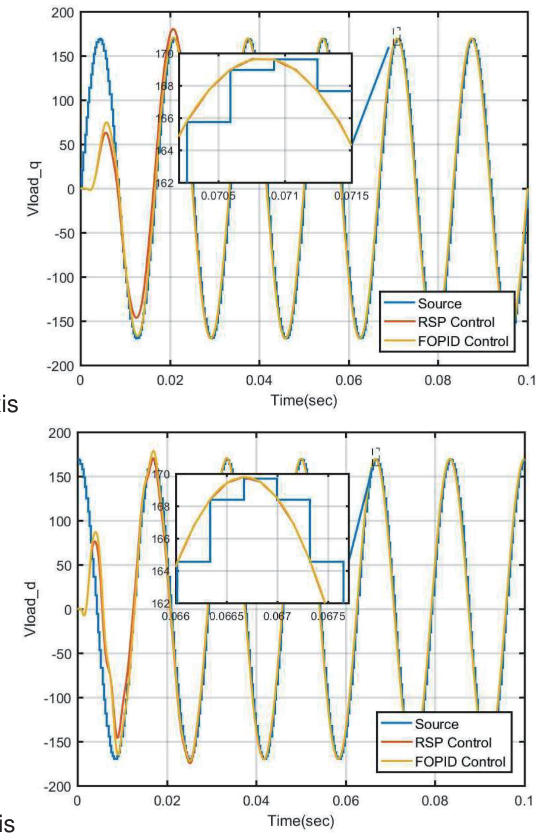

(a)q-axis

(b)d-axis

Fig. 6. Tracking dynamic of the reference voltage given by the Robustified Fractional Controller.

The parameters for each desired fractional weight are specified according to the recommendations provided above, as shown by the functions. Thus, the $NP - RS$ trade-off is well improved and the intended control objective has been met. Therefore, selecting these weights automatically is linked to determining the ideal parameters of the robust $FOPID$ voltage controller, whose transfer function is given by:

(28)
$$K_{ij}(s, x^{best}) = 1.8569 + \frac{3.1942}{s^{0.5412}} + 2.9501 s^{0.5313}$$

Where

(29)
$$\begin{cases} 0.01 \le K_p = 1.8569 \le 10 \\ 0.01 \le K_i = 3.1942 \le 10 \\ 0.01 \le K_d = 2.9501 \le 10 \\ 0.001 \le \lambda = 0.5412 \le 0.99 \\ 0.001 \le \mu = 0.5313 \le 0.99 \end{cases}$$

This all previous components of the resulting solutions confirms the well-chosen GA-based optimization procedure with no relaxation of lower and upper bounds.

The maximal singular values plots of the closed-loop system are depicted in Figures 4,5 . Figure 4 show that in the low frequency range ($\omega = 10^{-4} rad/s$), the better NP margin is obtained when the maximum singular values of the direct sensitivity matrix are small as possible. Also, Figure 4 shows that all singular values are bounded by $W_s^{-1}(s)$. Then, the offered robust control can satisfy the NP conditions. In addition, the control scheme offers a better RS margin in the high frequency range ($\omega = 10^8 rad/s$), where the complementary sensitivity matrix's maximal singular values has the steepest slope compared to slope of the initial conditions. The results demonstrate that the proposed controller-structure can successful the $NP - RS$ trade-off. As a result, as opposed to the RSP controller, the robust $FOPID$ provides greater robustness qualities. To substantiate the aforementioned results in the temporal domain, the Plant-model is exploited in the closed-loop system where three exogenous inputs.

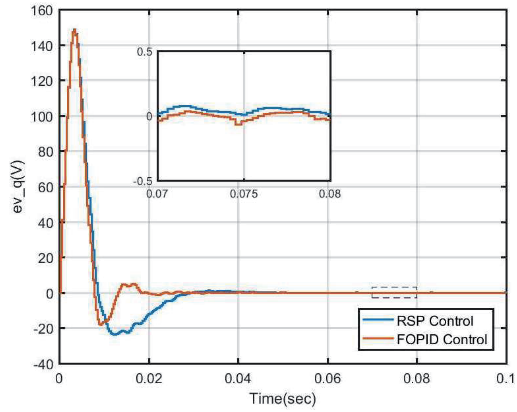

(a)q-axis

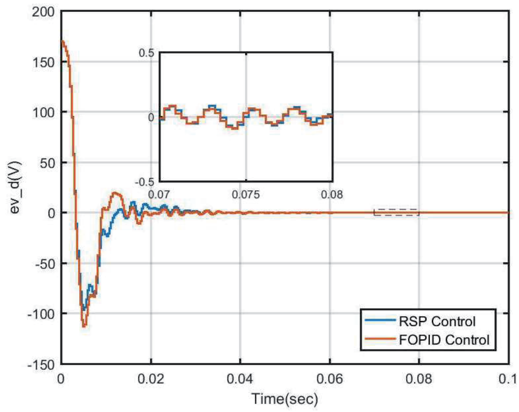

(a)q-axis

Fig. 7. The d-q axis voltage error of DG.

The desired source voltage always contains harmonics. For the DG-connected inverter system wish desired to eliminate third, fifth, and seventh harmonics. Figure 6 shows both load and reference voltages. As illustrated, the voltage signals converge to their nominal values. The figure shows that the voltage waveforms are only marginally affected by the load disturbance and revert to a steady state in a relatively short time. Therefore, Figure 7 show the obtained tracking error responses of the closed-loop system given by the RSP and robust adjustable fractional weights controllers. It can be observed that all controllers are coverging together properly .So that, the better tracking properties are ensured by the adjustable fractional weights controller, which is characterized by the fast attenuation dynamic of the harmonic voltage disturbances.

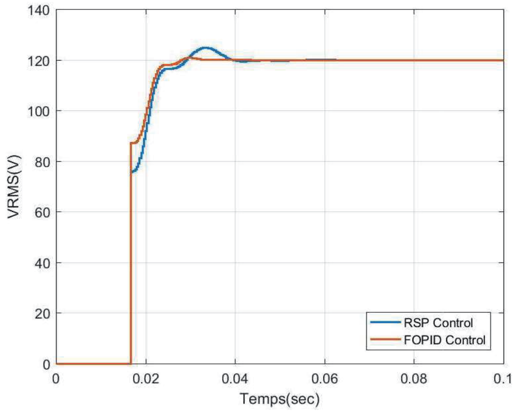

(a)VRMS

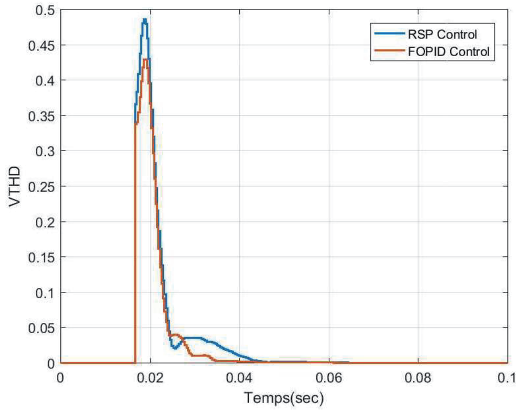

(a)VTHD

Fig. 8. Comparison of RMS and THD values of the load voltages.

The above-mentioned requirements are satisfied by the calibrated parameters of adjustable fractional weights, where the controller seems to be more sensitive to process perturbations. Steady state RMS output voltages and $THDs$ have been presented in Figure8. The proposed method achieves approximately zero steady state error and a THD of less than 0.5%. It can be observed that the RMS reveal about $2V$ deviations on each transient state.

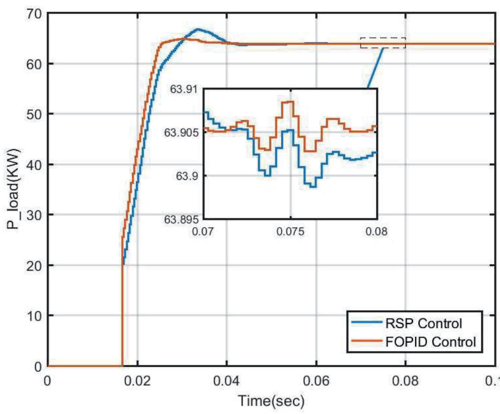

Fig. 9. Comparison results for real load powers.

The transient response of the control has been demonstrated and the harmonic distortion of DG voltage can be significantly suppressed under the adjustable fractional weights control mode which made the active power-sharing has acceptable accuracy and improves power quality of the DG unit as depicted in Figure 10. Ultimately, we can conclude that the proposed controller performs successfully to provide the both robust voltage control and active power sharing of DG-connected inverter in the presence of parametric uncertainties.

Conclusion

In this paper, a robust voltage H_∞ controller was proposed for a DG-connected inverter. To handle the uncertainties and to mitigate the impact of a voltage disturbance, this study was started by designing the theoretical concepts, including mathematical modelling of the DG-connected inverter, and Robust Servomechanism Problem design procedure for load voltage regulation as comparison controller. In addition, this study was followed by designing the proposed robust voltage H_∞ controller employing innovative structured H_∞ approaches. This study has confirmed by examination the three robustness settings NP, RS and trade-off among them for the voltage control loop. Moreover, the performance of the calibrated parameters of controller was evaluated under harmonic voltage disturbances based on temporal-domain simulations in the $MATLAB/Simulink$ environment and comparison with conventional Servomechanism control technique. Finally, as perceived by the results, the DG voltage maintained its stability when faced disturbances and the load efficiency were increased by $50Watts$. Future work might extend the previous study on an indispensable advance optimization tools to identify the parameters of both $FOPID$ model and Adjustable Fractional Weights.

***Authors**: PhD student, Oualid AMIEUR, University of Batna2 (Mostefa Ben Boulaïd), Department of Electrical Engineering, Laboratory LSPIE,*
E-mail: o.amieur@univ-batna2.dz
Orcid: 0000-0003-4838-8975.

REFERENCES

[1] VivekKumar and Ikbal Ali. Fractional order sliding mode approach for chattering free direct power control of dc/ac converter. *IET Power Electronics*, 12(13):3600–3610, 2019.
[2] ZoubirChelli, Abdelaziz Lakehal, Tarek Khoualdia, and Yacine Djeghader. Study on shunt active power filter control strategies of three-phase grid-connected photovoltaic systems. *Periodica Polytechnica Electrical Engineering and Computer Science*, 63(3), 2019.
[3] AliBidram and Ali Davoudi. Hierarchical structure of microgrids control system. *IEEE Transactions on Smart Grid*, 3(4):1963–1976, 2012.
[4] ManizaArmin, Mizanur Rahman, Md Mukidur Rahman, Subrata K Sarker, Sajal K Das, Md Rabiul Islam, Abbas Z Kouzani, and MA Parvez Mahmud. Robust extended h∞ control strategy using linear matrix inequality approach for islanded microgrid. *IEEE Access*, 8:135883–135896, 2020.
[5] HamidReza Baghaee, Mojtaba Mirsalim, Gevork B Gharehpetian, and Heidar Ali Talebi. A generalized descriptor-system robust h∞ control of autonomous microgrids to improve small and large signal stability considering communication delays and load nonlinearities. *International Journal of Electrical Power & Energy Systems*, 92:63–82, 2017.
[6] MohammadN Marwali, Min Dai, and Ali Keyhani. Robust stability analysis of voltage and current control for distributed generation systems. *IEEE Transactions on Energy Conversion*, 21(2):516–526, 2006.
[7] Tomas Hornik and Qing-Chang Zhong. A current-control strategy for voltage-source inverters in microgrids based on h∞ and repetitive control. *IEEE Transactions on Power Electron ics*, 26(3):943–952, 2010.
[8] LSedghi and Ahmad Fakharian. Robust voltage regulation in islanded microgrids: A lmi based mixed h2/h∞ control approach. In *2016 24th Mediterranean Conference on Control and Automation (MED)*, pages 431–436. IEEE, 2016.
[9] HiltonAbilio Grundling, Emerson Giovani Carati, and Jose Renes Pinheiro. Analysis and implementation of a modified robust model reference adaptive control with repetitive controller for ups applications. In *IECON'98. Proceedings of the 24th Annual Conference of the IEEE Industrial Electronics Society (Cat. No. 98CH36200)*, volume 1, pages 391–395. IEEE, 1998.
[10] ASheela, S Vijayachitra, and S Revathi. H-infinity controller for frequency and voltage regulation in grid-connected and is landed microgrid. *IEEJ Transactions on Electrical and Electronic Engineering*, 10(5):503–511, 2015.
[11] TS Lee, KS Tzeng, and MS Chong. Robust controller design for a single-phase ups inverter using μ-synthesis. *IEE Proceedings-Electric Power Applications*, 151(3):334–340, 2004.
[12] AbdelfatahM Mohamed. Modern robust control of a csi-fed induction motor drive system. In *Proceedings of the 1998 American Control Conference. ACC (IEEE Cat. No. 98CH36207)*, volume 6, pages 3803–3808. IEEE, 1998.
[13] Quang Linh Lam, Antoneta Iuliana Bratcu, and Delphine Riu. Robustness analysis of primary frequency h∞ control in standalone microgrids with storage units. *IFAC-PapersOnLine*, 49(27):123–128, 2016.
[14] JianZhao and Chao Li Wang. Frequency stability of microgrids based on h∞ methods. In *2016 35th Chinese Control Conference (CCC)*, pages 10079–10084. IEEE, 2016.
[15] ZMPe, PK Jain, and PC Sen. Robust controller design for high frequency resonant inverter system with voltage mode control. In *30th Annual Conference of IEEE Industrial Electronics Society, 2004. IECON 2004*, volume 1, pages 41–46. IEEE, 2004.
[16] Hassan Bevrani, Mohammad Ramin Feizi, and Sirwan Ataee. Robust frequency control in an islanded microgrid: H∞ and μ-synthesis approaches. *IEEE transactions on smart grid*, 7(2):706–717, 2015.
[17] MohsenHamzeh, Sepehr Emamian, Houshang Karimi, and Jean Mahseredjian. Robust control of an islanded microgrid under unbalanced and nonlinear load conditions. *IEEE Journal of Emerging and Selected Topics in Power Electronics*, 4(2):512–520, 2015.
[18] MohammadRaeispour, Hajar Atrianfar, Hamid Reza Baghaee, and Gevork B Gharehpetian. Robust sliding mode and mixed $h_2/h\infty$ output feedback primary control of ac microgrids. *IEEE Systems Journal*, 2020.
[19] SasanGholami, Sajeeb Saha, and Mohammad Aldeen. Robust multiobjective control method for power sharing among distributed energy resources in islanded microgrids with unbalanced and nonlinear loads. *International Journal of Electrical Power & Energy Systems*, 94:321–338, 2018.
[20] SalvatoreD'Arco, Jon Are Suul, and Olav Bjarte Fosso. Automatic tuning of cascaded controllers for power converters using eigenvalue parametric sensitivities. *IEEE Transactions on Industry Applications*, 51(2):1743–1753, 2014.
[21] MSedraoui, T Amieur, R Bachir Bouiadjra, and M Sahnoune. Robustified fractional-order controller based on adjustable fractional weights for a doubly fed induction generator. *Transactions of the Institute of Measurement and Control*, 39(5):660–674, 2017.
[22] Toufik Amieur, Abdelaziz Younsi, Mohammed Aidoud, Moussa Sedraoui, and Oualid Amieur. Design of robust fractional order pid controller using fractional weights in the mixed sensitivity problem. In *2017 14th International Multi-Conference on Systems, Signals & Devices (SSD)*, pages 549–553. IEEE, 2017.
[23] MohammadN Marwali and Ali Keyhani. Control of distributed generation systems-part i: Voltages and currents control. *IEEE Transactions on power electronics*, 19(6):1541–1550, 2004.
[24] MinDai, Mohammad Nanda Marwali, Jin-Woo Jung, and Ali Keyhani. A three-phase four-wire inverter control technique for a single distributed generation unit in island mode. *IEEE Transactions on power electronics*, 23(1):322–331, 2008.
[25] JiankunHu, Christian Bohn, and HR Wu. Systematic h∞ weighting function selection and its application to the real-time control of a vertical take-off aircraft. *Control Engineering Practice*, 8(3):241–252, 2000.
[26] GaryBalas, Richard Chiang, Andy Packard, and Michael Safonov. Robust control toolbox™ getting started guide. *The MathWorks, Incorporations. 3 Apple Hill Drive, Natick, MA 01760*, 2098, 2011.
[27] HOloomi and B Shafai. Weight selection in mixed sensitivity robust control for improving the sinusoidal tracking performance. In *42nd IEEE International Conference on Decision and Control (IEEE Cat. No. 03CH37475)*, volume 1, pages 300–305. IEEE, 2003.
[28] MGOrtega and FR Rubio. Systematic design of weighting matrices for the ∞ mixed sensitivity problem. *Journal of Process Control*, 14(1):89–98, 2004.
[29] NingZhang, Wei Gu, Haojun Yu, and Wei Liu. Application of coordinated sofc and smes robust control for stabilizing tie-line power. *Energies*, 6(4):1902–1917, 2013.